

## RADIATION AND MASS TRANSFER EFFECTS ON MHD FREE CONVECTION FLOW PAST AN IMPULSIVELY STARTED ISOTHERMAL VERTICAL PLATE WITH DISSIPATION

by

**Suneetha SANGAPATNAM, Bhaskar Reddy NANDANOOR,  
and Ramachandra Prasad VALLAMPATI**

Original scientific paper  
UDC: 536.255:66.021.3/4:517.96  
BIBLID: 0354-9836, 13 (2009), 2, 171-181  
DOI: 210.2298/TSCI0902171S

*This paper is focused on the study of effects of thermal radiation on the natural convective heat and mass transfer of a viscous, incompressible, gray absorbing-emitting fluid flowing past an impulsively started moving vertical plate with viscous dissipation. The governing boundary-layer equations are formulated in an  $(x, y, t)$  coordinate system with appropriate boundary conditions. The Rosseland diffusion approximation is used to analyze the radiative heat flux in the energy equation, which is appropriate for non-scattering media. The dimensionless governing equations are solved using an implicit finite-difference method of Crank-Nicolson type. The influence of Prandtl number, radiation-conduction parameter, thermal Grashof number, species Grashof number, Schmidt number, and Eckert number on the dimensionless velocity, temperature and concentration are studied. In addition the variation of the local and average skin-friction, Nusselt number, and Sherwood number for selected thermophysical parameters are computed and shown graphically. Increasing the Eckert number is seen to accelerate the flow. Thermal radiation reduces both velocity and temperature in the boundary layer. This model finds applications in solar energy collection systems, geophysics and astrophysics, aero space and also in the design of high temperature chemical process systems.*

Keywords: *thermal radiation, mass transfer, MHD, viscous dissipation, finite difference method*

### Introduction

Extensive research work has been published on an impulsively started vertical plate with different boundary conditions. Stokes [1] first presented an exact solution to the Navier-Stokes equation of the flow of a viscous incompressible fluid past an impulsively started infinite horizontal plate moving in its own plane. It is often called Rayleigh's problem in the literature. Stewartson [2] presented analytic solution to the viscous flow past an impulsively started semi-infinite horizontal plate. Hall [3] solved the problem of Stewartson by finite difference method of a mixed explicit-implicit type, which is convergent and stable. Soundalgekar [4] obtained the exact solution of the Stokes problem for the case of an infinite vertical plate, for the first time. Muthucumaraswamy [5] studied the natural convection on flow past an impulsively started vertical plate with variable surface heat flux.

Free convection flow involving coupled heat and mass transfer occurs frequently in nature and in industrial processes. A few representative fields of interest in which combined

heat and mass transfer plays an important role are designing of chemical processing equipment, formation and dispersion of fog, distribution of temperature and moisture over agricultural fields and groves of fruit trees, crop damage due to freezing, and environmental pollution. Das *et al.* [6] considered the mass transfer effects on the flow past an impulsively started infinite vertical plate with constant mass flux and chemical reaction. Muthucumaraswamy *et al.* [7] studied the problem of unsteady flow past an impulsively started isothermal vertical plate with mass transfer by an implicit finite difference method.

All these studies considered the fluid to be electrically non-conducting. However the flow of Newtonian electrically-conducting fluids is also of great interest in high speed aerodynamics, astronomical plasma flows, MHD boundary layer control, MHD accelerator technologies, *etc.* An excellent summary of applications can be found in [8]. Sacheti *et al.* [9] obtained an exact solution for unsteady MHD free convection flow on an impulsively started vertical plate with constant heat flux. Shankar *et al.* [10] discussed the effect of mass transfer on the MHD flow past an impulsively started infinite vertical plate with variable temperature or constant heat flux.

Thermal radiation in fluid dynamics has become a significant branch of the engineering sciences and is an essential aspect of various scenarios in mechanical, aerospace, chemical, environmental, solar power, and hazards engineering. For example Chang *et al.* [11] studied the effect of radiation heat transfer on free convection regimes in enclosures, with applications in geophysics and geothermal reservoirs. Hossain *et al.* [12] studied the radiation effects on mixed convection along a vertical plate with uniform surface temperature using the Rosseland flux model. Mosa [13] discussed one of the first models for combined radiative hydromagnetic heat transfer considering the case of free convective channel flows with an axial temperature gradient. Takhar *et al.* [14] analyzed the coupled magnetic field and thermal radiation effects in non-gray fluid boundary layer heat transfer, using a Runge-Kutta Merson quadrature. Abd El-Naby *et al.* [15] studied the radiation effects on MHD unsteady free-convection flow over vertical plate with variable surface temperature. Radiation and mass transfer effects on two dimensional flow past an impulsively started isothermal vertical plate was studied by Ramachandra Prasad *et al.* [16].

In all the investigations mentioned above, viscous mechanical dissipation is neglected. Such effects are important in geophysical flows and also in certain industrial operations and are usually characterized by the Eckert number. A number of authors have considered viscous heating effects on Newtonian flows. Mahajan *et al.* [17] reported the influence of viscous heating dissipation effects in natural convective flows, showing that the heat transfer rates are reduced by an increase in the dissipation parameter. Isreal-Cookey *et al.* [18] investigated the influence of viscous dissipation and radiation on unsteady MHD free convection flow past an infinite heated vertical plate in a porous medium with time dependent suction. Soundalgekar *et al.* [19] studied the finite difference analysis of mass transfer effects on flow past an impulsively started infinite isothermal vertical plate in a dissipative fluid. Very recently Zueco [20] used network simulation method [NSM] to study the effects of viscous dissipation and radiation on unsteady MHD free convection flow past a vertical porous plate.

However, the interaction of radiation with mass transfer of an electrically conducting dissipative fluid past an impulsively started isothermal vertical plate has received a little attention. Hence, the present study is attempted.

### Mathematical analysis

An unsteady two-dimensional laminar natural convection flow of a viscous, incompressible, electrically conducting, radiating fluid past an impulsively started semi-infinite verti-

cal plate in the presence of transverse magnetic field with viscous dissipation is considered. The fluid is assumed to be gray, absorbing-emitting but non-scattering. The x-axis is taken along the plate in the upward direction and the y-axis is taken normal to it. The fluid is assumed to be slightly conducting, and hence the magnetic Reynolds number is much less than unity and the induced magnetic field is negligible in comparison with the transverse applied magnetic field. Initially, it is assumed that the plate and the fluid are at the same temperature  $T'_\infty$  and concentration level  $C'_\infty$  everywhere in the fluid. At time  $t' > 0$ , the plate starts moving impulsively in the vertical direction with constant velocity  $u_0$  against the gravitational field. Also, the temperature of the plate and the concentration level near the plate are raised to  $T'_w$  and  $C'_w$ , respectively, and are maintained constantly thereafter. It is assumed that the concentration  $C'$  of the diffusing species in the binary mixture is very less in the comparison to the other chemical species, which are present, and hence the Soret and Dufour effects are negligible. It is also assumed that there is no chemical reaction between the diffusing species and the fluid. Then, under the above assumptions, in the absence of an input electric field, the governing boundary layer equations with Boussinesq's approximation are:

*Mass conservation*

$$\frac{\partial u}{\partial x} + \frac{\partial v}{\partial y} = 0 \quad (1)$$

*Momentum conservation*

$$\frac{\partial u}{\partial t'} + u \frac{\partial u}{\partial x} + v \frac{\partial u}{\partial y} = g\beta(T' - T'_\infty) + g\beta^*(C' - C'_\infty) + \nu \frac{\partial^2 u}{\partial y^2} - \frac{\sigma B_0^2}{\rho} u \quad (2)$$

*Energy conservation*

$$\frac{\partial T'}{\partial t'} + u \frac{\partial T'}{\partial x} + v \frac{\partial T'}{\partial y} = \alpha \frac{\partial^2 T'}{\partial y^2} - \frac{1}{\rho c_p} \frac{\partial q_r}{\partial y} + \frac{\nu}{c_p} \left( \frac{\partial u}{\partial y} \right)^2 \quad (3)$$

*Species conservation*

$$\frac{\partial C'}{\partial t'} + u \frac{\partial C'}{\partial x} + v \frac{\partial C'}{\partial y} = D \frac{\partial^2 C'}{\partial y^2} \quad (4)$$

The initial and boundary conditions are:

$$\begin{aligned} t' \leq 0: \quad & u = 0, \quad v = 0, \quad T' = T'_\infty, \quad C' = C'_\infty \\ t' > 0: \quad & u = u_0, \quad v = 0, \quad T' = T'_w, \quad C' = C'_w \quad \text{at } y = 0 \\ & u = 0, \quad T' = T'_\infty, \quad C' = C'_\infty \quad \text{at } x = 0 \\ & u \rightarrow 0, \quad T' \rightarrow T'_\infty, \quad C' \rightarrow C'_\infty \quad \text{as } y \rightarrow \infty \end{aligned} \quad (5)$$

where  $u$  and  $v$  are the velocity components in x- and y-directions, respectively,  $t'$  – the time,  $g$  – the acceleration due to gravity,  $\beta$  – the volumetric coefficient of thermal expansion,  $\beta^*$  – the volumetric coefficient of expansion with concentration,  $T'$  – the temperature of the fluid in the boundary layer,  $C'$  – the species concentration in the boundary layer,  $\nu$  – the kinematic viscosity,  $T'_w$  – the wall temperature,  $T'_\infty$  – the free stream temperature far away from the plate,  $C'_w$  – the concentration at the plate,  $C'_\infty$  – the free stream concentration far away from the plate,  $\sigma$  – the electrical conductivity,  $B_0$  – the magnetic induction,  $\rho$  – the density of the fluid,  $\alpha$  – the thermal diffusivity,  $c_p$  – the specific heat at constant pressure,  $q_r$  – the radiation heat flux, and  $D$  – the species diffusion coefficient.

Thermal radiation is assumed to be present in the form of a unidirectional flux in the y-direction *i. e.*,  $q_r$  (transverse to the vertical surface). By using the Rosseland approximation [21], the radiative heat flux  $q_r$  is given by:

$$q_r = -\frac{4\sigma_s}{3k_e} \frac{\partial T'^4}{\partial y} \quad (6)$$

where  $\sigma_s$  is the Stefan-Boltzmann constant and  $k_e$  – the mean absorption coefficient. It should be noted that by using the Rosseland approximation, the present analysis is limited to optically thick fluids. If temperature differences within the flow are sufficiently small, then eq. (6) can be linearized by expanding  $T'^4$  into the Taylor series about  $T'_\infty$ , which after neglecting higher order terms takes the form:

$$T'^4 \cong 4T'_\infty{}^3 T' - 3T'_\infty{}^4 \quad (7)$$

In view of eqs. (6) and (7), eq. (3) reduces to:

$$\frac{\partial T'}{\partial t'} + u \frac{\partial T'}{\partial x} + v \frac{\partial T'}{\partial y} = \alpha \frac{\partial^2 T'}{\partial y^2} + \frac{16\sigma_s T'_\infty{}^3}{3k_e \sigma c_p} \frac{\partial^2 T'}{\partial y^2} + \frac{v}{c_p} \left( \frac{\partial u}{\partial y} \right)^2 \quad (8)$$

Local and average skin-frictions are given, respectively, by:

$$\tau'_s = -\mu \left( \frac{\partial u}{\partial y} \right)_{y=0}, \quad \bar{\tau}L = \frac{-1}{L} \int_0^L \mu \left( \frac{\partial u}{\partial y} \right)_{y=0} dx \quad (9)$$

Local and average Nusselt numbers are given, respectively, by:

$$\text{Nu}_x = \frac{-x \left( \frac{\partial T'}{\partial y} \right)_{y=0}}{T'_w - T'_\infty}, \quad \bar{\text{Nu}}_L = - \int_0^L \left[ \frac{\left( \frac{\partial T'}{\partial y} \right)_{y=0}}{T'_w - T'_\infty} \right] dx \quad (10)$$

Local and average Sherwood numbers are given, respectively, by:

$$\text{Sh}_x = \frac{-x \left( \frac{\partial C'}{\partial y} \right)_{y=0}}{C'_w - C'_\infty}, \quad \bar{\text{Sh}}_L = - \int_0^L \left[ \frac{\left( \frac{\partial C'}{\partial y} \right)_{y=0}}{C'_w - C'_\infty} \right] dx \quad (11)$$

Defining:

$$X = \frac{xu_0}{v}, \quad Y = \frac{yu_0}{v}, \quad t = \frac{t'u_0^2}{v}, \quad U = \frac{u}{u_0}, \quad V = \frac{v}{u_0} \quad (12)$$

$$\text{Gr} = \frac{v g \beta (T'_w - T'_\infty)}{u_0^3}, \quad \text{Gm} = \frac{v g \beta^* (C'_w - C'_\infty)}{u_0^3}, \quad N = \frac{k_e k}{4\sigma_s T'_\infty{}^3}, \quad M = \frac{\sigma B_0^2 v}{u_0^2}$$

$$T = \frac{T' - T'_\infty}{T'_w - T'_\infty}, \quad C = \frac{C' - C'_\infty}{C'_w - C'_\infty}, \quad \text{Pr} = \frac{v}{\alpha}, \quad \text{Sc} = \frac{v}{\alpha}, \quad \text{Ec} = \frac{u_0^2}{c_p (T'_w - T'_\infty)}$$

where  $k$  is the thermal conductivity.

Equations (1), (2), (8), and (4) are reduced to the following non-dimensional form:

$$\frac{\partial U}{\partial X} + \frac{\partial V}{\partial Y} = 0 \quad (13)$$

$$\frac{\partial U}{\partial t} + U \frac{\partial U}{\partial X} + V \frac{\partial U}{\partial Y} = GrT + GmC + \frac{\partial^2 U}{\partial Y^2} - MU \tag{14}$$

$$\frac{\partial T}{\partial t} + U \frac{\partial T}{\partial X} + V \frac{\partial T}{\partial Y} = \frac{1}{Pr} \left( 1 + \frac{4}{3N} \right) \frac{\partial^2 T}{\partial Y^2} + Ec \left( \frac{\partial u}{\partial y} \right)^2 \tag{15}$$

$$\frac{\partial C}{\partial t} + U \frac{\partial C}{\partial X} + V \frac{\partial C}{\partial Y} = \frac{1}{Sc} \frac{\partial^2 C}{\partial Y^2} \tag{16}$$

where Gr, Gm,  $M$ ,  $N$ , Pr, Ec, and Sc are the thermal Grashof number, solutal Grashof number, magnetic parameter, radiation parameter, Prandtl number, Eckert number, and Schmidt number, respectively.

The corresponding initial and boundary conditions are:

$$\begin{aligned} t \leq 0: & \quad U = 0 \quad V = 0, \quad T = 0, \quad C = 0 \\ t > 0: & \quad U = 1, \quad V = 0, \quad T = 1, \quad C = 1 \quad \text{at } Y = 0 \\ & \quad U = 0, \quad T = 0, \quad C = 0 \quad \text{at } X = 0 \\ & \quad U \rightarrow 0, \quad T \rightarrow 0 \quad \text{as } Y \rightarrow \infty \end{aligned} \tag{17}$$

Using the non-dimensional quantities (12), local as well as average values of skin friction, Nusselt number, and Sherwood number are:

$$\tau_X = \frac{\tau'}{\rho u_0^2} = - \left( \frac{\partial U}{\partial Y} \right)_{Y=0}, \quad \bar{\tau} = - \int_0^1 \left( \frac{\partial U}{\partial Y} \right)_{Y=0} dX \tag{18}$$

$$Nu_X = -X \left[ \frac{\left( \frac{\partial T}{\partial Y} \right)_{Y=0}}{T_{Y=0}} \right], \quad \bar{Nu} = - \int_0^1 \left[ \frac{\left( \frac{\partial T}{\partial Y} \right)_{Y=0}}{T_{Y=0}} \right] dX \tag{19}$$

$$Sh_X = -X \left[ \frac{\left( \frac{\partial C}{\partial Y} \right)_{Y=0}}{C_{Y=0}} \right], \quad \bar{Sh} = - \int_0^1 \left[ \frac{\left( \frac{\partial C}{\partial Y} \right)_{Y=0}}{C_{Y=0}} \right] dX \tag{20}$$

### Numerical technique

The unsteady coupled non-linear eqs. (13)-(16) with the conditions (17) are solved by employing an implicit finite difference method of Crank-Nicolson type. The region of integration is considered as a rectangle with sides  $X_{max} (=1)$  and  $Y_{max} (=14)$ , where  $Y_{max}$  corresponds to  $Y = \infty$  which lies very well outside the momentum, thermal and concentration boundary layers. The maximum value of  $Y$  is chosen as 14 after some preliminary investigations, so that the last two of the boundary conditions (17) are satisfied. We now divide  $X$ - and  $Y$ -directions into  $M$  and  $N$  grid-spacing, respectively. The mesh sizes are taken as  $\Delta X = 0.05$ ,  $\Delta Y = 0.25$ , and  $\Delta t = 0.01$ .

The finite difference equations corresponding to eqs. (13)-(16) are:

$$\begin{aligned} & \frac{U_{i,j}^{n+1} - U_{i,j}^{n+1} + U_{i,j}^n - U_{i-1,j}^n + U_{i,j-1}^{n+1} - U_{i-1,j-1}^{n+1} + U_{i,j-1}^n - U_{i-1,j-1}^n}{4\Delta X} + \\ & + \frac{V_{i,j}^{n+1} - V_{i,j-1}^{n+1} + V_{i,j}^n - V_{i,j-1}^n}{2\Delta Y} = 0 \end{aligned} \tag{21}$$

$$\begin{aligned} \frac{U_{i,j}^{n+1} - U_{i,j}^n}{\Delta t} + U_{i,j}^n \frac{U_{i,j}^{n+1} - U_{i-1,j}^{n+1} + U_{i,j}^n - U_{i-1,j}^n}{2\Delta X} + V_{i,j}^n \frac{U_{i,j+1}^{n+1} - U_{i,j-1}^{n+1} + U_{i,j+1}^n - U_{i,j-1}^n}{4\Delta Y} = \\ \frac{2}{\text{Gr} \frac{T_{i,j}^{n+1} + T_{i,j}^n}{2} + \text{Gm} \frac{C_{i,j}^{n+1} + C_{i,j}^n}{2}} + \\ + \frac{U_{i,j-1}^{n+1} - 2U_{i,j}^{n+1} + U_{i,j+1}^{n+1} + U_{i,j-1}^n - 2U_{i,j}^n + U_{i,j+1}^n}{2(\Delta Y)^2} - M \frac{U_{i,j}^{n+1} + U_{i,j}^n}{2} \end{aligned} \quad (22)$$

$$\begin{aligned} \frac{T_{i,j}^{n+1} - T_{i,j}^n}{\Delta t} + U_{i,j}^n \frac{T_{i,j}^{n+1} - T_{i-1,j}^{n+1} + T_{i,j}^n + T_{i-1,j}^n}{2\Delta X} + V_{i,j}^n \frac{T_{i,j} - T_{i,j-1}^{n+1} + T_{i,j+1}^n - T_{i,j-1}^n}{4\Delta Y} = \\ = \frac{1}{\text{Pr}} \left( 1 + \frac{4}{3N} \right) \frac{T_{i,j-1}^{n+1} - 2T_{i,j}^{n+1} + T_{i,j+1}^{n+1} + T_{i,j}^n - 2T_{i,j}^n + T_{i,j+1}^n}{2(\Delta Y)^2} + \text{Ec} \left[ \frac{U_{i,j+1}^n - U_{i,j}^n}{\Delta Y} \right] \end{aligned} \quad (23)$$

$$\begin{aligned} \frac{C_{i,j}^{n+1} - C_{i,j}^n}{\Delta t} + U_{i,j}^n \frac{C_{i,j}^{n+1} - C_{i-1,j}^{n+1} + C_{i,j}^n - C_{i-1,j}^n}{2\Delta X} + V_{i,j}^n \frac{C_{i,j+1}^{n+1} - C_{i,j-1}^{n+1} + C_{i,j+1}^n - C_{i,j-1}^n}{4\Delta Y} = \\ = \frac{1}{\text{Sc}} \frac{C_{i,j-1}^{n+1} - 2C_{i,j}^{n+1} + C_{i,j+1}^{n+1} + C_{i,j-1}^n - 2C_{i,j}^n + C_{i,j+1}^n}{2(\Delta Y)^2} \end{aligned} \quad (24)$$

Now during the computations, in any one time step, the coefficients  $U_{i,j}^n$  and  $V_{i,j}^n$  appearing in the difference equations are treated as constants. The values of  $C$ ,  $T$ ,  $U$ , and  $V$  are known at all grid points at  $t = 0$  from the initial conditions. The values of  $C$ ,  $T$ ,  $U$ , and  $V$  at time level  $n + 1$  using the known values at previous time level  $n$  are calculated as follows. The finite difference eq. (24) at every internal nodal point on a particular  $i$ -level constitute a tridiagonal system of equations, which is solved by using Thomas algorithm as discussed in Carnahan *et al.* [22]. Thus, the values of  $C$  are known at every internal nodal point on a particular  $i$  at  $(n + 1)^{\text{th}}$  time level. Similarly, the values of  $T$  are calculated from eq. (23). Using the values of  $C$  and  $T$  at  $(n + 1)^{\text{th}}$  time level in eq. (22), the values of  $U$  at  $(n + 1)^{\text{th}}$  time level are found in similar manner. Then the values of  $V$  are calculated explicitly using the eq. (21) at every nodal point at particular  $i$ -level at  $(n + 1)^{\text{th}}$  time level. This process is repeated for various  $i$ -levels. Thus the values of  $C$ ,  $T$ ,  $U$ , and  $V$  are known, at all grid points in the rectangular region at  $(n + 1)^{\text{th}}$  time level. Computations are carried out until the steady-state is reached. The steady-state solution is assumed to have been reached, when the absolute differences between the values of  $U$  as well as temperature  $T$  and concentration  $C$  at two consecutive time steps are less than  $10^{-5}$  at all grid points.

The local truncation error is  $O(\Delta t^2 + \Delta Y^2 + \Delta X)$  and it tends to zero as  $\Delta t$ ,  $\Delta Y$ , and  $\Delta X$  tend to zero. Hence the scheme is compatible. The finite difference scheme is unconditionally stable as discussed in [21]. Compatibility and stability ensures the convergence of the scheme.

## Results and discussion

Extensive computations have been performed for the effects of the controlling thermo fluid and hydrodynamic parameters on the dimensionless velocities ( $U$ ), temperature ( $T$ ) and concentration ( $C$ ), and also on the local and average skin frictions ( $\tau_x$ ,  $\bar{\tau}$ ), local and average Nusselt numbers ( $\text{Nu}_x$ ,  $\bar{\text{Nu}}$ ) and local and average Sherwood numbers ( $\text{Sh}_x$ ,  $\bar{\text{Sh}}$ ). Default values of the parameters are: conduction radiation parameter ( $N$ ) *i. e.* stark number = 3, thermal Grashof

number ( $Gr$ ) = 2, species Grashof number ( $Gm$ ) = 2, Prandtl number ( $Pr$ ) = 0.71 (air), Schmidt number ( $Sc$ ) = 0.6 ( $H_2O$ ), Eckert number ( $Ec$ ) = 0.001, and magnetic parameter ( $M$ ) = 1.0. All the graphs therefore correspond to these values unless specifically indicated on the appropriate graph.

The transient velocity profiles of the present problem are compared with that of Prasad *et al.* [16] in fig.1, and they are found to be in good agreement.

Figure 2 illustrates the effects of  $Gr$ ,  $Gm$ , and  $M$  on the dimensionless transient velocity profiles *vs.*  $Y$  (transverse co-ordinate).  $Gr$  signifies the relative effect of the thermal buoyancy force to the viscous hydrodynamic force in the boundary layer regime. An increase in  $Gr$  or  $Gm$  induces a rise in the steady-state velocity profiles. There is a rapid rise in the velocity near the wall and then the velocity descends smoothly towards zero. An increase in  $M$  reduces the velocity. The application of a transverse magnetic field to an electrically conducting fluid gives rise to a resistive type of force called Lorentz force. This force has the tendency to slow down the fluid. This trend is evident from fig. 2.

The effect of conduction-radiation parameter,  $N$  (*i. e.* stark number) on the velocity and temperature variations along the vertical surface *i. e.* in the stream wise direction is depicted in figs. 3(a) and 3(b). As  $N$  increases, considerable reduction is observed in velocity and temperature profiles from the peak value at the wall ( $Y=0$ ) across the boundary layer regime to the free stream ( $Y \rightarrow \infty$ ), at which the velocity and temperature are negligible for any value of  $N$ . It is also observed that reduction in velocity and temperature are accompanied by simultaneous reductions in both velocity and thermal boundary layers. All profiles decay asymptotically to zero in the free stream.

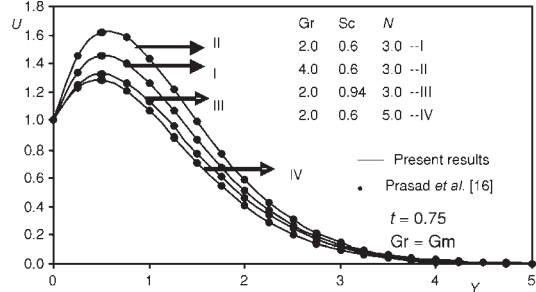


Figure 1. Transient velocity profiles at  $X = 1.0$  for different  $Gr$ ,  $Sc$ , and  $N$

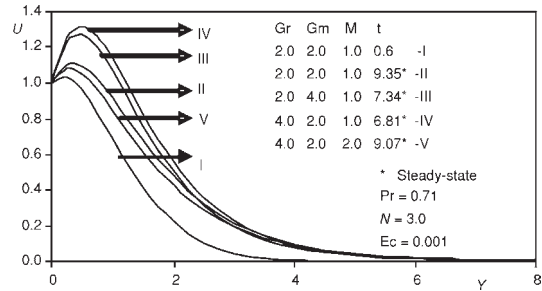


Figure 2. Effect of  $Gr$ ,  $Gm$ , and  $M$  on velocity profiles

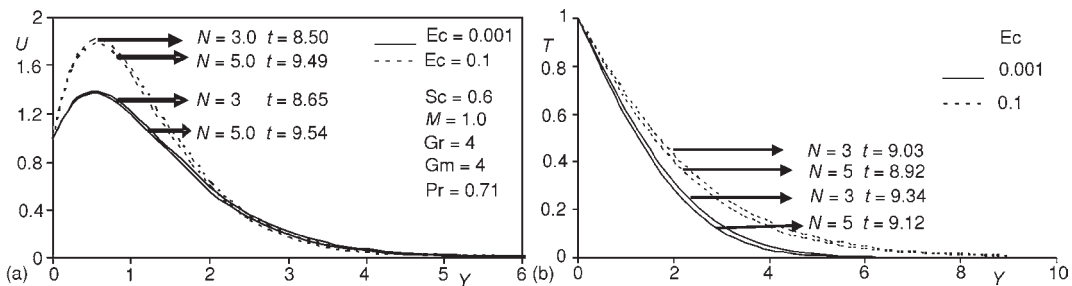


Figure 3. (a) Steady-state velocity profiles at  $X = 1.0$  for different  $N$ ; (b) Temperature profiles at  $X = 1.0$  for different  $N$



The influences of the foreign mass and radiation parameter on the transient velocity and concentration profiles are shown in figs. 4(a) and 4(b). It is observed that the velocity and concentrations decrease due to an increase in  $Sc$  or  $N$ . Figure 4(a) shows that concentration decreases rapidly, with an increase in  $Sc$ , as  $Sc$  corresponds to a decrease in the chemical molecular diffusivity *i. e.* less diffusion therefore takes place by mass transport. The dimensionless concentration profiles also decay from a maximum concentration of 1 at  $Y = 0$  (the wall boundary condition) to zero in the free stream.

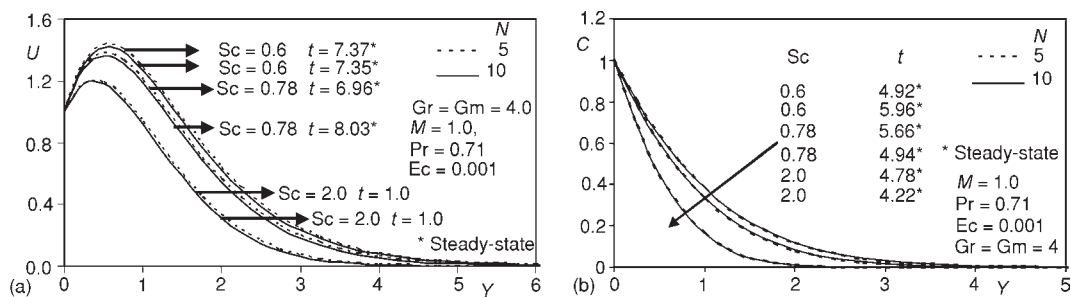


Figure 4. (a) Velocity profiles at  $X = 1.0$  for different  $Sc$  and  $N$ ; (b) Concentration profiles at  $X = 1.0$  for different  $Sc$

The influence of  $Pr$  on the velocity and temperatures are shown in figs. 5(a) and 5(b).  $Pr$  encapsulates the ratio of momentum diffusivity to thermal diffusivity. The numerical results show that an increase in the Prandtl number results in a decrease of the thermal boundary layer thickness and in general lower average temperature within the boundary layer. The reason is that smaller values of  $Pr$  are equivalent to increasing the thermal conductivity of the fluid, and therefore heat is able to diffuse away from the heated surface more rapidly than higher values of  $Pr$ . Hence in the case of smaller  $Pr$ , the thermal boundary layer is thicker and the rate of heat transfer is reduced. Therefore an increase in  $Pr$  reduces velocity. It is noticed that both the velocity and temperatures decrease as  $Pr$  increases, as expected. The profiles also steepen and intersect the abscissa faster for large  $Pr$ , *i. e.*, velocities and temperatures across the boundary layer (normal to the wall) reach zero faster.

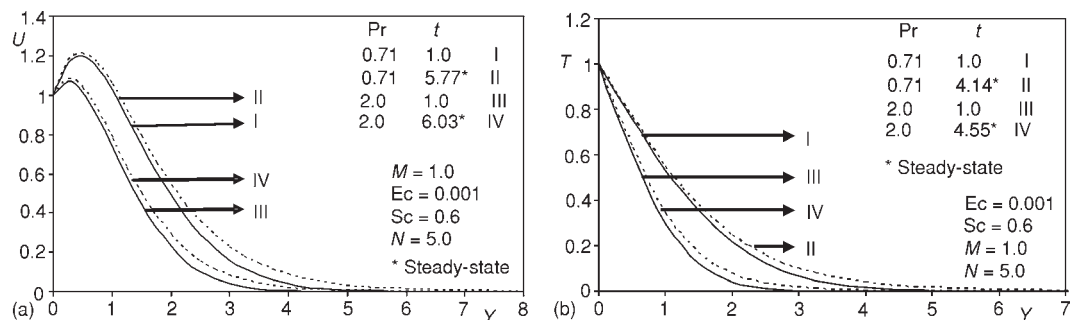
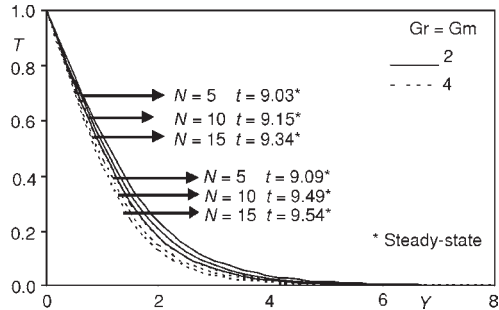


Figure 5. (a) Velocity profiles for different values of  $Pr$ ; (b) Temperature profiles at  $X = 1.0$  for different values of  $Pr$

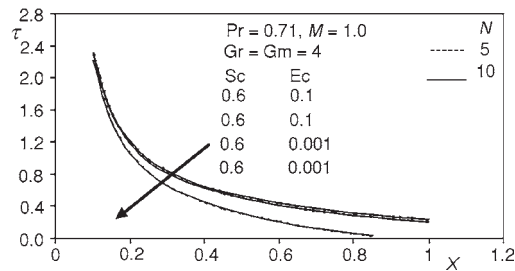




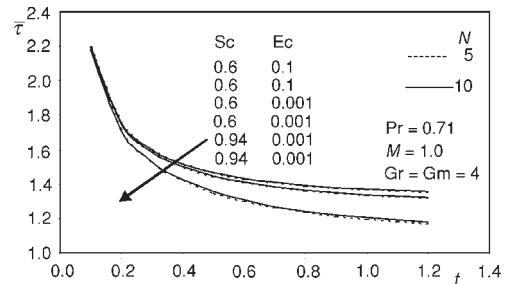
**Figure 6. Steady-state temperature profiles at  $X = 1.0$  for different  $Gr$ ,  $Gm$ , and  $N$**

Figure 6 shows that the temperature decreases with the increasing values of  $Gr$  or  $Gm$ . It can also be seen that the time required to reach the steady-state temperature is more at higher values of  $N(=15)$ , as compared to lower values of  $N(=5)$ .

Shear stress (local skin friction)  $\tau_x$  profiles are shown in fig. 7. It is observed that the local skin-friction increases as  $Ec$  or  $N$  increases, whereas it decreases as  $Sc$  increases. The average skin-friction rises due to a rise in  $Ec$  or  $N$ , whereas it decreases with an increase in  $Sc$ , which are shown in fig. 8.



**Figure 7. Local skin friction**



**Figure 8. Average skin friction**

The Local Nusselt number  $Nu_x$  for different  $Gr$ ,  $Gm$ ,  $Ec$ , and  $N$  are shown in fig. 9. It is noticed that  $Nu_x$  increases with an increase in  $Gr$  or  $Gm$  or  $N$ , whereas it decreases with greater viscous dissipative heat. The average Nusselt number decreases with greater viscous dissipative heat and increases with an increase in  $Sc$  or  $N$ , which are plotted in fig. 10.

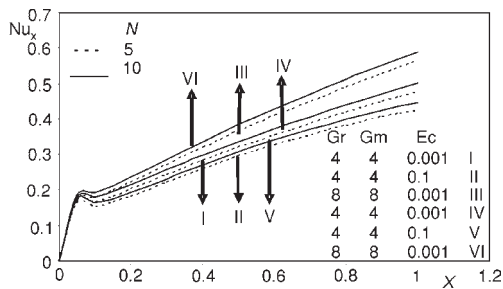


**Figure 9. Local Nusselt number**

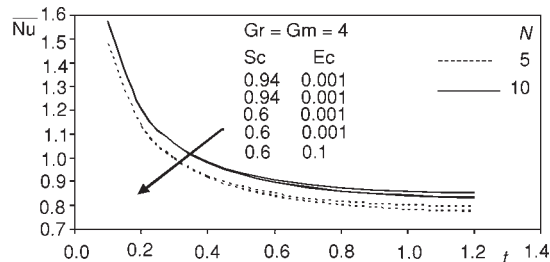


**Figure 10. Average Nusselt number**

From figs. 11 and 12, it is found that the local and average Sherwood numbers increase slightly due to the presence of viscous dissipative heat, but there is a substantial rise in their values with an increase in the value of Schmidt number. It is also observed that local Sherwood number decreases due to an increase in  $Gr$  or  $N$ . But the average Sherwood number is not affected by  $Gr$ , whereas it increases with an increase in  $N$ .

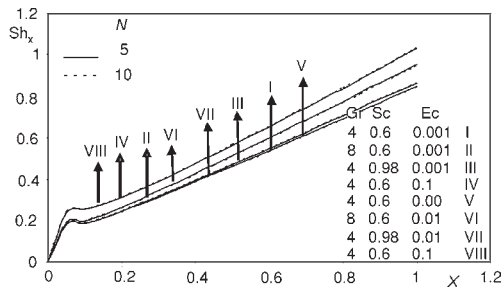


Figure 11. Local Sherwood number

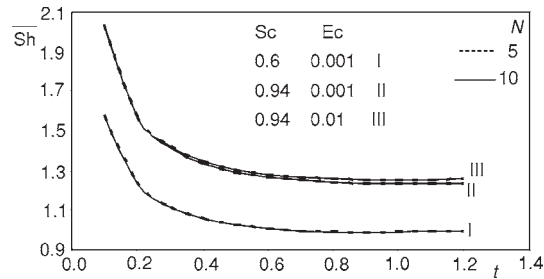


Figure 12. Average Sherwood number

## Conclusions

A mathematical model has been presented for the radiative-convective flow in a gray absorbing-emitting fluid adjacent to a vertical impulsively started surface. The Rosseland diffusion flux model has been used to simulate radiative flux. A family of governing partial differential equations is solved by an implicit finite difference scheme of Crank-Nicolson type. The results are obtained for different values of conduction-radiation parameter ( $N$ ), thermal Grashof number ( $Gr$ ), species Grashof number ( $Gm$ ), Prandtl number ( $Pr$ ), Schmidt number ( $Sc$ ), Eckert number ( $Ec$ ), and also time on the pertinent dependent variables. It has been shown that:

- increasing  $N$  or  $Gr$  or  $Gm$  or  $Pr$  reduces temperature, whereas a rise in  $Sc$  increases temperature along the wall and transverse to the wall,
- a rise in  $N$  causes a large reduction in transient velocity  $U$ ,
- a rise in  $Ec$  induces a substantial rise in both velocity and temperature,
- an increase in  $N$  causes a small decrease in concentration  $C$ ,
- the local and average skin-friction decreases with an increase in  $Gr$  or  $Gm$  and increases with the increase in  $N$ ,
- the local and average Nusselt numbers increase with an increase in  $N$  and decrease with an increase in  $Ec$ , and
- the Local and average Sherwood numbers increase with an increase in  $Ec$  or  $Sc$ .

## References

- [1] Stokes, G. G., On the Effect of Internal Friction of Fluids on the Motion of Pendulums, *Camb. Phil. Trans IX* (1851), 2, pp. 8-106
- [2] Stewartson, K., On the Impulsive Motion of a Flat Plate in a Viscous Fluid, *Quarterly Journal of Mechanics and Applied Mathematics, IV* (1951), 2, pp.182-198
- [3] Hall, M. G., The Boundary Layer over an Impulsively Started Flat Plate, *Proc. Roy. Soc. A, 310* (1969), 1502, pp .401-414
- [4] Soundalgekar, V. M., Free Convection Effects on the Stokes Problem for Infinite Vertical Plate, *ASME, J. Heat Transfer, 99c* (1977), 6, pp. 499-501
- [5] Muthucumaraswamy, R., Natural Convection on Flow Past an Impulsively Started Vertical Plate with Variable Surface Heat Flux, *Far East Journal of Applied Mathematics, 14* (2004), 1, pp. 99-109
- [6] Das, U. N., Deka, R. K., Soundalgekar, V. M., Effects of Mass Transfer on Flow Past an Impulsively Started Infinite Vertical Plate with Constant Heat Flux and Chemical Reaction, *Forschung im Ingenieurwesen, 60* (1994), 10, pp. 284-287
- [7] Muthucumaraswamy, R., Ganesan, P., Unsteady Flow Past an Impulsively Started Vertical Plate with Heat and Mass Transfer, *Heat and Mass Transfer, 14* (1998), 2, pp. 187-193
- [8] Huges, W. F., Young, F. J., *The Electro-Magneto-Dynamics of Fluids*, John Wiley & Sons, New York, USA, 1966

- [9] Sacheti, N. C., Chandran, P., Singh, A. K., An Exact Solution for Unsteady MHD Free Convection Flow with Constant Heat Flux, *Int. Comm. Heat Mass Transfer*, 21 (1994), 1, pp. 131-142
- [10] Shankar, B., Kishan, N., The Effect of Mass Transfer on the MHD Flow Past an Impulsively Started Infinite Vertical Plate with Variable Temperature or Constant Heat Flux, *Journal of Energy, Heat and Mass Transfer*, 19 (1997), 3, pp. 273-278
- [11] Chang, L. C., Yang, K. T., Lloyd, J. R., Radiation Natural Convection Interactions in Two Dimensional Complex Enclosures, *ASME J. Heat Transfer*, 105 (1983), 1, pp. 89-95
- [12] Hossain, M. A., Takhar, H. S., Radiation Effects on Mixed Convection along a Vertical Plate with Uniform Surface Temperature, *J. Heat and Mass Transfer*, 31 (1996), 4, pp. 243-248
- [13] Mosa, M. F., Radiative Heat Transfer in Horizontal MHD Channel Flow with Buoyancy Effects and an Axial Temperature Gradient, Ph. D. thesis, Mathematics Department, Bradford University, Bradford, U. K., 1979
- [14] Takhar, H. S., Gorla, R. S. R., Soundalgekar, V. M., Radiation Effects on MHD Free Convection Flow of a Radiating Fluid Past a Semi-Infinite Vertical Plate, *Int. J. Numerical Methods for Heat and Fluid Flow*, 6 (1996), 1, pp.77-83
- [15] Abd El-Naby, M. A., *et al.*, Finite Difference Solution of Radiation Effects on MHD Free Convection Flow over a Vertical Plate with Variable Surface Temperature, *J. Appl. Math.*, 2 (2003), 2, pp. 65-86
- [16] Ramachandra Prasad, V., Bhaskar Reddy, N., Muthucumaraswamy, R., Radiation and Mass Transfer Effects on Two-Dimensional Flow Past an Impulsively Started Infinite Vertical Plate, *Int. J. Thermal Sciences*, 46 (2007), 12, pp. 1251-1258
- [17] Mahajan, R. L., Gebhart, B. B., Viscous Dissipation Effects in Buoyancy-Induced Flows, *Int. J. Heat Mass Transfer*, 32 (1989), 7, pp. 1380-1382
- [18] Israel-Cookey, C., Ogulu, A., Omubo-Pepple, V. M., Influence of Viscous Dissipation on Unsteady MHD Free Convection Flow Past an Infinite Vertical Plate in Porous Medium with Time-Dependent Suction, *Int. J. Heat Mass Transfer*, 46 (2003), 13, pp. 2305-2311
- [19] Soundalgekar, V. M., Hiremath, S. V., Finite Difference Analysis of Mass Transfer Effects on Flow Past an Impulsively Started Infinite Isothermal Vertical Plate in Dissipative Fluid, *Astro Physics and Space Science*, 95 (1983), 2, pp.163-173
- [20] Zueco Jordan, J., Network Simulation Method Applied to Radiation and Dissipation Effects on MHD Unsteady Free Convection over Vertical Porous Plate, *Appl. Math., Modelling*, 31 (2007), 20, pp. 2019-2033
- [21] Brewster, M. Q., Thermal Radiative Transfer and Properties, John Wiley & Sons, New York, USA, 1992
- [22] Carnahan, B., Luther, H. A., Willkes, J. O., Applied Numerical Methods, John Wiley & Sons, New York, USA, 1969

Author's affiliations:

S. Suneetha, N. Bhaskar Reddy  
Department of Mathematics,  
Spi Venkateswara University, India

V. Ramachandra Prasad (corresponding author)  
Department of Mathematics, MITS, Madanapalle, A. P., India  
E-mail: rcpmaths@yahoo.com

Paper submitted: July 6, 2008  
Paper revised: February 17, 2009  
Paper accepted: February 27, 2009